Light inducible protein degradation in *E. coli* with LOVtag

Nathan Tague[1,2], Cristian Coriano-Ortiz[1,2], Michael B. Sheets[1,2], Mary J. Dunlop[1,2*]

[1] Department of Biomedical Engineering, Boston University, Boston, MA, USA 02215
[2] Biological Design Center, Boston University, Boston, MA, USA 02215
* Corresponding author: mjdunlop@bu.edu

Abstract
Molecular tools for optogenetic control allow for spatial and temporal regulation of cell behavior. In particular, light controlled protein degradation is a valuable mechanism of regulation because it can be highly modular, used in tandem with other control mechanisms, and maintain functionality throughout growth phases. Here, we engineered LOVtag, a protein tag that can be appended to a protein of interest for inducible degradation in *Escherichia coli* using blue light. We demonstrate the modularity of LOVtag by using it to tag a range of proteins, including the LacI repressor, CRISPRa activator, and the AcrB efflux pump. Additionally, we demonstrate the utility of pairing the LOVtag with existing optogenetic tools to enhance performance by developing a combined EL222 and LOVtag system. Finally, we use the LOVtag in a metabolic engineering application to demonstrate post-translational control of metabolism. Together, our results highlight the modularity and functionality of the LOVtag system, and introduce a powerful new tool for bacterial optogenetics.

Introduction
Currently, the most widely used optogenetic systems in bacterial synthetic biology rely on transcription to modulate gene expression. Light responsive transcription factors allow genes of interest to be controlled modularly without having to re-engineer promoters. These tools have provided a valuable means to probe regulatory networks (Dessauges et al., 2022; Harrigan et al., 2018; Lugagne and Dunlop, 2019; Olson et al., 2014). However, these networks can be governed by complex control, where post-transcriptional and post-translational mechanisms work in concert with transcriptional regulation (Chubukov et al., 2014; Link et al., 2013; Mahmoud and Chien, 2018). Light responsive regulators that act beyond transcription are necessary to more fully mimic natural biology and have the potential to improve upon current deficits of transcriptional control. In synthetic contexts, transcriptional regulation suffers from limited response dynamics. In the case of gene activation, the time delay inherent to transcription and translation, which reaches steady-state after >1.5 hours for inducible promoters (Golding et al., 2005; Olson et al., 2014), restricts the speed at which an input signal can be actuated. More problematically, in the case of gene deactivation, decreasing protein abundance is limited by cell division-based dilution or natural protein half-lives, which are in the range of 5-20 hours for the majority of proteins in *E. coli* (Maurizi, 1992). When cells are growing in exponential phase the effective degradation rate of these long-lived proteins is the cell cycle time, which is on the order of 0.5 hours. However, at high cell densities, such as during stationary phase, slow growth rates result in protein half-lives on the scale of 10s of hours (Maier et al., 2011). Subpopulations of cells in stationary phase have been reported to proliferate, however these growing subpopulations are small compared to non-growing cells and add to heterogeneous protein half-lives within the population (Jõers et al., 2020),

making it challenging to reliably remove these proteins. It should be noted that a proportion of proteins are actively degraded during slow growth, but these represent the minority in *E. coli* (Gupta et al., 2022). This is a critical issue for metabolic engineering where chemical production is typically carried out at stationary phase in two-stage fermentations (Lalwani et al., 2018).

Post-translational optogenetic control has the potential to address some of the shortcomings of transcriptional regulation because post-translational control mechanisms can function independently of growth-based dilution. Existing approaches to post-translational optogenetic control include the use of light inducible dimers in split protein systems (Baumschlager et al., 2017; Kawano et al., 2015; Nihongaki et al., 2015), domain insertions with light controlled allosteric domains (Dagliyan et al., 2016; Gil et al., 2020), and membrane-confined functional control (Strickland et al., 2012; Wang et al., 2016). These approaches, however, suffer from a lack of modularity, which is a key benefit of the transcriptional control approaches. Split protein systems and domain insertions require extensive engineering for each protein of interest and solutions for a given protein are unlikely to map to proteins with different structures. Likewise, localization-based approaches are only applicable to a small subset of proteins that have location dependent function, such as transcription factors that require nuclear localization (Yumerefendi et al., 2018).

Protein degradation offers potential as a modular post-translational mechanism of control. Endogenous proteolytic machinery is necessary for proteome homeostasis and acts as a global regulatory system (Mahmoud and Chien, 2018). Targeted proteolysis has proven useful in many synthetic biology applications in both eukaryotic and prokaryotic organisms (Andersen et al., 1998; Cameron and Collins, 2014; McGinness et al., 2006; Morreale et al., 2022; Trauth et al., 2019) In eukaryotic cells, light dependent protein degradation has been demonstrated using various mechanisms (Bonger et al., 2014; Deng et al., 2020; Liu et al., 2020; Renicke et al., 2013; Xue et al., 2019). For example, Bonger *et al.* utilized the LOV2 domain of *Avena sativa* phototropin 1 (*As*LOV2), to achieve light dependent protein degradation in mammalian cells (Bonger et al., 2014). LOV2 is a blue-light responsive protein that is widely used in optogenetic tools (Pudasaini et al., 2015). LOV2 contains a core Per-Arnt-Sim (PAS) domain surrounded by N- and C-terminal α-helices. Upon blue light illumination, the LOV2 protein undergoes a conformational change where the C-terminal Jα helix reversibly unfolds and becomes unstructured (Halavaty and Moffat, 2007; Harper et al., 2003; Yamamoto et al., 2009). Incorporation of a degradation-targeted peptide sequence into the C-terminal resulted in light dependent protein degradation in yeast (Renicke et al., 2013).

However, the bacterial proteasome differs from the eukaryotic proteasome in many ways (Mahmoud and Chien, 2018; Schrader et al., 2009). The bacterial proteasome includes several proteases with divergent targeting behaviors and does not utilize ubiquitin as a generalized modification to trigger degradation (Finley, 2009). In bacteria, protein targeting for degradation is predominantly dependent on primary amino acid sequence as opposed to a ubiquitin-like appendage and, apart from certain well-studied cases, the rules governing sequence recognition of bacterial degrons are not fully understood (Baker and Sauer, 2006; Striebel et al., 2009). Because of these complexities, light dependent degradation systems for bacteria have lagged behind their eukaryotic counterparts, where interaction of a ubiquitin ligase with a defined degron can be used as a control mechanism (Bondeson et al., 2022). Nevertheless, optogenetic degradation remains a

key target for bacterial synthetic biology applications. In principle, an optogenetic degradation system could be fast-acting, modular, and interface with endogenous proteasome machinery. These features would provide a straightforward way of adding dynamic control to any protein of interest, complementing existing transcriptional tools for optogenetic control of gene expression. One recent system developed by Komera *et al.* utilizes a light responsive split TEV protease to expose or remove constitutively active degradation tags in *E. coli* (Komera et al., 2022). Although this system achieves protein degradation in response to light, it acts indirectly through activation of an exogenous protease. A simpler approach where the degradation tag itself is light responsive would streamline this by eliminating the need for multiple exogenous components.

Here, we develop LOVtag, a modular protein tag based on the *As*LOV2 protein that is conditionally degraded in response to blue light in *E. coli*. We demonstrate that attaching this tag to a protein of interest confers light dependent protein instability. We show the modularity of LOVtag by incorporating it into multiple proteins with widely varying function, converting them all into optogenetically controlled systems without the need for extensive protein engineering. In addition, through photocycle stabilizing mutations, we create a version of the LOVtag that responds to infrequent exposure to blue light. We also demonstrate that our degradation tag can be used in concert with other optogenetic systems for multi-layer control by using EL222, a blue light responsive system for transcriptional control, together with the LOVtag. Lastly, we incorporate optogenetic degradation into a metabolically engineered strain to control production of octanoic acid. Overall, this work introduces a new bacterial optogenetic tool that overcomes the drawbacks of transcriptional control by providing post-translational degradation, while avoiding the substantial protein engineering required for alternative post-translational control mechanisms.

Results

Design and characterization of the AsLOV2-based degradation tag

The *E. coli* proteasome consists of five AAA+ proteases and is continuously active, either degrading misfolded proteins for quality control or balancing regulatory protein levels (Mahmoud and Chien, 2018). We set out to exploit endogenous proteasome activity in order to design a light responsive protein tag. To do this, we took insight from studies related to native protein quality control. In bacteria, peptides from stalled ribosomes are targeted for degradation through interaction with a tmRNA that appends a short amino acid sequence, known as an SsrA tag, to the C-terminal end of the incomplete protein (Keiler, 2015). The *E. coli* SsrA tag has been studied extensively and is known to interact with the unfoldases ClpX and ClpA (Flynn et al., 2001; Gottesman et al., 1998). Addition of the SsrA peptide sequence to exogenous proteins targets them for degradation by the host proteasome. SsrA mediated degradation has proven useful in synthetic gene circuit function and biochemical production (Elowitz, 2000; Gurbatri et al., 2020; Stricker et al., 2008; Torella et al., 2013; Ye et al., 2021). A recent structural study of ClpX interacting with the SsrA tag from Fei *et al*. demonstrated that in order for ClpX to unfold a tagged protein, the C-terminal tail needs to be unstructured and sufficiently long to fit into the ClpX pore (Fei et al., 2020). We reasoned that the mechanism of *As*LOV2, in which the C-terminal Jα helix becomes unstructured upon blue light absorption, could be utilized to provide light inducible protein degradation.

Biochemical studies have probed the amino acid sequence of the SsrA tag and its role in degradation targeting. Flynn *et al*. demonstrated that ClpA and ClpX unfoldases interact with overlapping residues within the SsrA sequence and that the last three amino acids (L-A-A) are particularly important for successful degradation (Flynn et al., 2001). Importantly, they showed that mutation of the leucine in the C-terminal 'L-A-A' lowers unfoldase affinity but does not hinder degradation completely. We noticed that the C-terminal amino acid sequence of the *As*LOV2 domain, comprised of residues 404-546 of *Avena sativa* phototropin 1, are 'E-A-A' at positions 541-543 (Fig. 1a). The dark state structure of *As*LOV2 (PDB: 2V1A) shows that these three amino acids and K544 complete the folded Jα helix (Fig. 1b). A truncation of residues 544-546 leaves the Jα helix largely intact and the resulting C-terminal 'E-A-A' remains caged as part of the folded helix. We hypothesized that this truncation would be stable in the dark state as a consequence of 'E-A-A' caging and unstable in the light state due to Jα helix unfolding and exposure of an unstructured degradation tag.

Optogenetic systems have used the *As*LOV2 domain in *E. coli*, however, it is often appended N-terminally or internally to another protein (Li et al., 2022; Strickland et al., 2008). To the best of our knowledge, wild type or truncated *As*LOV2, with its C-terminal end exposed, have not been used for proteolytic degradation in bacterial cells. To test the stability of C-terminal *As*LOV2 in *E. coli* in response to light, we constructed a plasmid where we used an IPTG-inducible promoter to control the expression of mCherry translationally fused to *As*LOV2 (Fig. 1c). In this construct, the full C-terminal sequence is intact so unfoldases are not expected to have good access for protein degradation. Consistent with this, induction of mCherry-*As*LOV2(546) with IPTG increased expression of the fusion construct, and 465 nm blue light induction resulted in only a modest decrease in expression (Fig. 1d). Next, we tested a version of the construct where three amino acids were truncated to expose the C-terminal 'E-A-A', *As*LOV2(543). This construct destabilized the protein fusion as predicted, resulting in significantly lower expression compared to the non-truncated version (Fig. 1d). However, counter to our expectations, we observed only a modest decrease in expression upon blue light induction.

While *As*LOV2 switches from mostly folded in the dark state to mostly unfolded in the light state, both states are present at an equilibrium with or without light (Yao et al., 2008). Due to the suboptimal equilibrium of native *As*LOV2, dark state undocking and unfolding of the Jα helix is a common issue in *As*LOV2-based optogenetic tools, and many studies have aimed at improving the dynamic range of *As*LOV2 (Guntas et al., 2015; Lungu et al., 2012; Strickland et al., 2012, 2010; Wang et al., 2016). Guntas *et al*., performed phage display on an *As*LOV2-based protein that incorporates a caged peptide sequence in the Jα helix. They identified a variant with 11 amino acid substitutions with much tighter dark state caging, called iLID. Interestingly, several of these mutations do not have a direct interaction with the caged peptide, but instead are located at the hinge loop connecting the PAS domain to the Jα helix or in the PAS domain itself (Fig. S1). Guntas *et al*. further characterized amino acid substitutions and determined several that did not affect caging or dynamic range if reverted (F502Q, H521R, and C530M). We focused on the mutations found to result in tighter dark state caging (L493V, H519R, V520L, D522G, G528A, E537F, N538Q, and D540A), and reasoned that this set should stabilize the Jα helix irrespective of the caged peptide. Thus, we next constructed a variant of *As*LOV2 with these eight mutations, which we denote as *As*LOV2*.

To test whether these mutations are beneficial in the context of protein stabilization, we fused *As*LOV2*(546) or *As*LOV2*(543) to mCherry (Fig. 1c). Non-truncated *As*LOV2*(546) expressed highly with the addition of IPTG, but blue light did not result in a decrease in mCherry levels, consistent with lack of access by proteases (Fig. 1d). In contrast, the truncated version containing the mutations, AsLOV2*(543), displayed the desired light induced degradation, expressing highly in the dark and exhibiting 11.5x lower expression in response to blue light (Fig. 1d). We also confirmed that *As*LOV2*(543) expression was decreased in response to light without any IPTG induction (Fig. S2). Further, *As*LOV2*(543) is destabilized in proportion to light intensity (Fig. 1e). We conducted experiments to identify the mechanism underlying *As*LOV2*(543) degradation and found evidence that ClpA is involved, and other proteases and unfoldases play complementary roles (Supplementary Text, Fig. S3-6). A potential concern is that light induced disorder of the Jα helix could result in a decrease in solubility and aggregation of mCherry-*As*LOV2*(543). To rule this out as the cause of the fluorescence decrease, we captured microscopy images of cells in dark and light conditions. The imaging confirmed a light-dependent decrease in mCherry expression without the formation of visible protein aggregates (Fig. S7). Thus, the AsLOV2*(543) variant provides blue light dependent protein degradation; we refer to this variant as the LOVtag.

Modularity of the LOVtag

Post-translational control of protein function typically requires extensive protein engineering for each use case. Degradation tags, by contrast, offer post-translational control that theoretically requires little to no protein engineering and is protein agnostic. To test the modularity of the LOVtag, we incorporated optogenetic control into three systems with highly diverse functions and relevance to synthetic biology and biotechnology applications: the LacI repressor, CRISPRa activation, and the AcrB efflux pump.

First, we sought to test whether the LOVtag could be fused to transcription factors to enable light dependent regulation. The LacI repressor is one of the most commonly used chemically inducible systems in synthetic biology. We translationally fused the LOVtag to LacI and paired it with a reporter where the LacUV5 promoter controls expression of mCherry (Fig. 2a). Our results show that light exposure successfully increased mCherry expression (Fig. 2b). Light induced mCherry expression did not achieve the full levels provided with saturating IPTG induction, however we still observed a notable increase. We tested an alternative strategy for further improving de-repression, which suggested that the discrepancy between IPTG versus light dependent induction likely stems from the delay in LacI degradation compared to the rapid allosteric action of IPTG (Supplementary Text, Fig. S8).

Next, we incorporated the LOVtag into the SoxS-based bacterial CRISPRa activation system (Dong et al., 2018). In this system, a scaffold RNA, which is a modified gRNA containing an MS2 stem loop, is used to localize dCas9 and the transcriptional activator SoxS, which is fused to an MS2 coat protein (MCP). We translationally fused the LOVtag to the MCP-SoxS protein, such that in the dark CRISPRa will be active and light exposure relieves activation (Fig. 2c). In the original system, MCP-SoxS expression is anhydrotetracycline (aTc) inducible. This induction system in not amenable to blue light stimulation because aTc is photosensitive (Baumschlager et al., 2020). Thus, we changed the MCP-SoxS construct to an IPTG inducible promoter prior to blue light experiments (Fig. S9a, Table S1, Table S2). We confirmed that the promoter switch

maintained CRISPRa activity (Fig. S9b). Fusing the LOVtag to the activator component indeed relieved CRISPRa activity, resulting in a decrease in expression under blue light stimulation (Fig. 2d).

We also added the LOVtag to the endogenous membrane protein AcrB. This represents a challenging test case for degrading a native protein. The AcrAB-TolC complex is a multidrug efflux pump with clinical relevance due to its role in antibiotic tolerance and resistance acquisition (El Meouche and Dunlop, 2018; Lizarralde-Guerrero and Taraveau, 2021; Okusu et al., 1996). AcrAB-TolC has also been utilized in metabolic engineering as a mechanism to pump out toxic chemical products and boost strain performance (Dunlop et al., 2011; Fisher et al., 2014). However, inducible control of AcrB is challenging because cell viability is sensitive to overexpression (Turner and Dunlop, 2015). Optogenetic transcriptional control systems have high dynamic ranges but do not operate in the low expression ranges relevant to very potent proteins such as AcrB. Light based degradation is well suited for this challenge because it works by decreasing expression, allowing the upper bound of expression to be determined by the promoter.

Previous work from Chai *et al*. demonstrated that AcrB can be targeted for proteolysis by fusing an SsrA tag to the C-terminal (Chai et al., 2016). Degradation is possible because the C-terminal end of AcrB is on the cytoplasmic side of the inner membrane and can interact with cytoplasmic unfoldases (Du et al., 2014). Therefore, we reasoned that fusing the LOVtag to AcrB would result in light inducible degradation that disrupts activity of the AcrAB-TolC complex (Fig. 2e). To determine if activity of the AcrAB-TolC complex was successfully disrupted by light, we performed a minimum inhibitory concentration (MIC) test using the antibiotic chloramphenicol. AcrAB-TolC is known to increase tolerance to chloramphenicol (Okusu et al., 1996). We transformed a construct containing tagged AcrB into cells lacking the endogenous *acrB* gene (Δ*acrB*). When kept in the dark, Δ*acrB* cells with AcrB-LOVtag showed comparable chloramphenicol tolerance to wild type cells (Fig. 2f-g). Blue light stimulation, in contrast, sensitized the Δ*acrB* + AcrB-LOVtag strain to chloramphenicol compared to both wild type and Δ*acrB* + AcrB-LOVtag kept in the dark (Fig. 2f-g). This suggests that the LOVtag successfully targets AcrB for degradation in a light dependent fashion in a range that is physiologically relevant. When compared to Δ*acrB* without any AcrB complementation, the blue light exposed cells do not reach the same level of chloramphenicol sensitivity, likely due to basal levels of efflux pump expression from AcrB-LOVtag relative to the knockout (Fig. S10).

Tuning frequency response of the LOVtag

Light inducible systems have the potential to respond to the frequency of light exposure. Frequency dependent tools can allow optogenetic circuits to be multiplexed beyond limited wavelength options and add a layer of logic to optogenetic circuits (Benzinger et al., 2022). With added logic operations, optogenetic circuits could perform complex signal processing, analogous to those demonstrated with multiplexed chemically inducible circuits (Shin et al., 2020), while allowing dynamic light inputs. Additionally, higher sensitivity LOVtags would also be useful in bioreactor settings, where poor light penetration into dense cultures is a feasibility concern. With these use cases in mind, we sought to investigate and alter the LOVtag frequency response.

LOV domains utilize a flavin cofactor to absorb light. In the case of *As*LOV2, the cofactor responsible for light absorption is flavin mononucleotide (FMN). A cysteine residue in *As*LOV2 forms a reversible covalent bond with FMN, which initiates broader conformation change. A full photocycle of *As*LOV2 consists of absorption of a photon, covalent bond formation with cysteine 450, Jα helix destabilization and unfolding, decay of the cysteine-FMN bond, and Jα helix refolding (Swartz et al., 2001). Previous studies have determined the dynamics of bond formation and the time delay of Jα helix refolding. Further, mutations have been found that stabilize or destabilize the light state conformation (Christie et al., 2007; Kawano et al., 2013; Zayner et al., 2013). In the context of the LOVtag, the time needed for the Jα helix to refold, known as the reversion time, likely determines degradation characteristics (Fig. 3a). In principle, the time spent in the light state dictates the amount of time the protein is susceptible to degradation and, therefore, would impact the frequency response given variable light inputs.

To test the effect of LOVtag refolding dynamics, we illuminated cells with 5 second pulses of blue light followed by variable length dark periods to allow Jα helix refolding (Fig. 3b). While holding the blue light duration fixed, we tested dark periods ranging from 475 seconds (5:475 seconds on:off, frequency of 0.01 seconds^{-1}) to 5 seconds (5:5 seconds on:off, frequency of 0.5 seconds^{-1}). We first tested the frequency response of the original LOVtag (Fig. 3c). The response is in line with known refolding dynamics of *As*LOV2 (Li et al., 2020), where over 50% degradation is only achieved at high frequencies (0.5 seconds^{-1}, which corresponds to 5:5 seconds on:off). Next, we tested a LOVtag variant that contains a slow-photocycle mutation, V416I (Zoltowski et al., 2009). This amino acid substitution has been shown to increase the dark state recovery from 8 seconds to 84 seconds *in situ* (Li et al., 2020). Indeed, for LOVtag (V416I) over 50% degradation was achieved at medium frequencies (0.04 seconds^{-1}, which corresponds to 5:120 seconds on:off) (Fig. 3c). This variant offers the potential for better performance in settings where increased light sensitivity is preferred, such as bioreactors.

Integrating the LOVtag with EL222 for multi-layer control

Another attractive aspect of post-translational optogenetic control is that it can integrate with existing systems that act at the transcriptional or translational level. Adding control at multiple layers has been shown to enhance the performance and robustness of natural and synthetic systems (Alon, 2007; Hasenjäger et al., 2019; Szydlo et al., 2022). One commonly used system for optogenetic transcriptional control is the EL222 protein. EL222 is a blue light responsive LOV protein that dimerizes and binds DNA upon light exposure (Zoltowski et al., 2013). In bacteria, EL222 can be used as a transcriptional repressor or activator depending on the placement of its binding site in the promoter (Ding et al., 2020; Jayaraman et al., 2016). We chose to combine the transcriptional repression of EL222 with the LOVtag. In this arrangement, the systems work synergistically to decrease gene expression in response to blue light using simultaneous transcriptional repression and protein degradation (Fig. 4a).

To test the performance of this combined optogenetic circuit, we created a construct in which the mCherry-LOVtag fusion protein is driven by a constitutively active promoter containing an EL222 binding site (P_{EL222}). We tested the light response of mCherry-LOVtag expression with and without EL222 present (Fig. 4b). As expected, mCherry expression decreased in response to light even without EL222 present, representing the sole action of the degradation tag. However, multi-layer

control resulted in a faster decrease in expression in response to light and reached significantly lower levels compared to the degradation tag alone. The fold change decrease in expression was improved from 15x for just the LOVtag to 269x when both systems were combined.

Optogenetic control of octanoic acid production

We next sought to apply the LOVtag to a metabolic engineering task, as we envision that post-translational control will be especially advantageous in these biotechnology applications. Transcriptional control alone is particularly problematic in a metabolic engineering setting because chemical production is typically carried out at stationary phase with slow growth rates, meaning that proteins expressed at basal levels will accumulate in production settings. Therefore, dynamic control using transcriptional optogenetic systems alone will only allow protein levels to increase or plateau. However, a prerequisite for dynamic control of metabolic pathways is that enzyme levels can be modulated to turn off production. Thus, the LOVtag protein degradation system offers excellent potential for control in metabolic engineering applications.

As a proof of concept, we chose to control the enzyme *Cp*FatB1 with the LOVtag or the EL222-LOVtag circuit. *Cp*FatB1 is an acyl-ACP thioesterase from *Cuphea palustris* that primarily catalyzes octanoyl-ACP to produce octanoic acid. Octanoic acid is a valuable medium chain oleochemical with limited natural sources (Sarria et al., 2017). Specifically, we expressed the catalytically enhanced mutant from Hernandez-Lozada, *et al.*, *Cp*FatB1.2-M4-287, which we denote here as *Cp*FatB1* (Hernández Lozada et al., 2018). This enzyme interfaces with the endogenous fatty acid synthesis pathway in *E. coli* to produce free fatty acids (Fig. 5a). In this pathway, the carbon tail of an acyl-ACP moiety is elongated two carbons at a time. *Cp*FatB1* specifically catalyzes C8-ACPs, which results in production of free octanoic acid. Importantly, since *Cp*FatB1* is very catalytically active, low levels of expression are optimal for production and strains with high expression exhibit a growth defect (Hernández Lozada et al., 2018). Therefore, to dynamically control *Cp*FatB1* activity in cells, expression must be controlled in a low range, which is particularly challenging in stationary phase.

A first step towards optogenetically controlling this metabolic pathway is to demonstrate that enzyme levels can be modulated between expression levels that are relevant to endpoint titers. If expression can only oscillate between high and medium expression levels, dynamic light control will not be effective. To test whether we could effectively stunt *Cp*FatB1* activity, we controlled enzyme expression using only EL222 repression, only LOVtag degradation, or EL222 and LOVtag throughout at 24 hour fermentation period (Fig. 5b). The EL222 only control did not significantly decrease octanoic acid production with light, demonstrating the shortcomings of solely transcriptional control at stationary phase. In contrast, both the LOVtag alone and the LOVtag with EL222 resulted in a significant decrease in octanoic acid in the continuous light condition. Thus, protein degradation is needed to effectively shunt the metabolic pathway during stationary phase.

Clearly, decreasing titers is not the overall goal in metabolic engineering. However, the ability to control expression at relevant ranges throughout stationary phase represents an important stepping stone to investigate dynamic control schemes or feedback control that may lead to enhanced strain performance.

Discussion

Here, we developed and characterized the LOVtag, which provides blue light inducible protein degradation, offering unique advantages as a tool for bacterial synthetic biology. Protein degradation offers a mode of control that is currently limited in the bacterial optogenetic toolkit. The bacterial light responsive degradation system from Komera *et al.* accomplishes protein degradation indirectly through an exogenous split protease (Komera et al., 2022). In comparison, in our approach the degradation tag itself is light responsive and does not require extra components, making it straightforward to incorporate. In this study, we showed that the truncated *As*LOV2 protein can be fused to the C-terminal end of various proteins to destabilize them and then target them for degradation. The addition of stabilizing mutations from iLID result in low basal activity in the dark, with strong switching in response to light. Aside from creating a light-responsive degradation tag, the effectiveness of these stabilizing mutations may serve to improve the switch-like behavior in many other *As*LOV2-based systems.

We demonstrated the modularity of the LOVtag by incorporating it into three distinct contexts with little to no fine tuning. Each system, the LacI repressor, CRISPRa activation, and the AcrB efflux pump, were converted to optogenetically controlled by simply tagging the protein with the LOVtag. This modularity mimics the ease of use of transcriptional optogenetic systems, which only require a change of the promoter. However, incorporating light control at the protein level simplifies this process because expression levels can remain in their native, or previously fine-tuned, context. For example, the AcrB efflux pump is beneficial to the cell only at low expression levels, as higher expression negatively impacts cell health (Turner and Dunlop, 2015). To maintain low exogenous expression, researchers typically rely on leaky expression from inducible systems or chromosomal integration (El Meouche and Dunlop, 2018; Teelucksingh et al., 2022). Addition of the LOVtag has the benefit that it does not disrupt the system at the transcriptional level and allows protein levels to be decreased further. This configuration is especially beneficial for proteins that require low expression, as transcriptional optogenetic systems often suffer from leaky basal expression. The LOVtag provides a design that can work with endogenous expression levels, circumventing this issue. In this study, we focused on proteins expressed on plasmids from synthetic promoters. However, we anticipate the LOVtag can be useful in systems biology contexts where natural promoters linked to endogenous gene networks are best left untouched. In this case, the LOVtag can add the ability to optogenetically manipulate genes while keeping them in their native gene regulatory context.

Since degradation occurs post-translationally, the LOVtag can easily be integrated with existing optogenetic systems to enhance their function. We demonstrated this by combining the LOVtag with the EL222 repression system, showing that the synergistic action of transcriptional repression and degradation results in a drastic increase in the dynamic range, owing to the much lower off-state under light illumination. In this configuration, EL222 and the LOVtag work coherently to decease expression. However, the LOVtag can potentially be incorporated into activating systems incoherently to create dynamic functionality, such as pulse generators and inverters (Benzinger et al., 2022).

Throughout this study, we performed experiments using low copy number plasmids that result in moderate expression levels of a given protein of interest. While this is a common use case for synthetic biology, degradation as the sole mode of gene expression control may be limiting when proteins are at very high expression levels. As an ATP-dependent process that utilizes a finite pool of proteolytic machinery, degradation rates can saturate at sufficiently high expression levels. Furthermore, using protein degradation as the sole mode of gene expression control is wasteful in some contexts. Constitutive transcription and translation of a gene followed by degradation utilizes valuable cellular resources, which is an important consideration in metabolic engineering. To avoid this type of energetic waste, we envision the LOVtag could be used in concert with other modes of regulation, as we demonstrated with EL222. In addition, it is unclear whether the LOVtag is compatible with other prokaryotic (including mitochondrial) proteasomes. Future studies focused on the portability of the LOVtag may address this question and potentially lead to further mechanistic insight.

In summary, the LOVtag offers a straightforward route for introducing optogenetic control of protein degradation in *E. coli*. By lowering the barrier to entry for incorporating light responsiveness into a protein of interest, we envision that systems typically studied with chemical induction or constitutive expression can now be controlled optogenetically without extensive fine-tuning. Furthermore, the LOVtag can act as a circuit enhancer when incorporated into existing optogenetic systems to increase functionality and robustness.

Methods

Strains and plasmids

We used *E. coli* BW25113 as the wild type strain. All knockout strains are from the Keio collection (Baba et al., 2006), which were derived from BW25113. We used golden gate cloning to create all plasmid constructs (Engler et al., 2008) (Table S1). The IPTG inducible constructs were derived from pBbS5c-mRFP1 from the BglBrick plasmid library (Lee et al., 2011). In the constitutive version of the mCherry-AsLOV2 variants, we swapped the IPTG inducible promoter with a constitutive promoter, P_{W7} (5'-ttatcaaaaagagtattgaaataaagtctaacctataggaagattacagccatcgagagggacacggcgaa-3'). We used this constitutive version for microscopy and the protease knockout studies; all other experiments used the IPTG inducible promoter.

In all cases of protein fusions to *As*LOV2 variants, a five amino acid GS linker of 'S-S-G-S-G' was used between the protein of interest and the LOVtag. In the LacI-LOVtag experiments, pBbS5c-mCherry was also used as the backbone, but with the LOVtag sequence cloned after the *lacI* gene instead of *mCherry*. In the LacI-LOVtag experiment to test the impact of basal LacI, pBbS5c-LacI-LOVtag-mCherry was co-transformed with pBbAa-LacI-Decoy from Wang and Tague *et al.* (Wang et al., 2021).CRISPRa constructs were based on the MS2-SoxS system from Dong *et al*. (Dong et al., 2018). The J106 gRNA sequence from Dong *et al*. was used to target dCas9 upstream mRFP1 under control of the minimal J1 promoter. This gRNA plasmid was constructed using the golden gate assembly method to replace the targeting sequence in the pCD061 backbone (Addgene #113315). The mRFP1 reporter plasmid was derived from pJF076Sa (Addgene #113322) by replacing the ampicillin resistance gene with a kanamycin resistance gene from the BglBrick library. MS2-SoxS-LOVtag was expressed from a variant of pJF093 (Addgene

#113323). TetR and its corresponding promoter driving expression of MS2-SoxS were replaced with the LacI-P_{Trc} inducible system from pBbA1c-mRFP1 from the BglBrick library (Lee et al., 2011). The inducer was changed to IPTG because aTc is sensitive to blue light (Baumschlager et al., 2020). The LOVtag was added to this construct with a C-terminal fusion to SoxS. Plasmids containing *acrAB* were built from pBbA5k-acrAB from El Meouche *et al*. (El Meouche and Dunlop, 2018). The FLP recombination protocol from Datsenko and Wanner was used to cure the kanR cassette from the genome of the Δ*acrB* strain (Keio collection, JW0451)(Datsenko and Wanner, 2000).

The slow photocycle variant of the LOVtag, V416I, was constructed using site directed mutagenesis of Valine at amino acid position 416.

EL222 was synthesized by IDT (Coralville, IA) and plasmids were constructed to mimic EL222 repression systems from Jayaraman *et al*. (Table S1) (Jayaraman et al., 2016). A variant of the promoter $P_{BLrep\text{-}v1}$ from Ding *et al*., P_{raB} was used in all EL222 experiments and we refer to it in figures as P_{EL222} (Ding et al., 2020). Plasmid pBbE5k-P_{EL222}-mCherry-LOVtag was co-transformed with pEL222, which constitutively expresses EL222 (Table S2).

For octanoic acid production experiments, the coding sequence of *Cp*FatB1.2-M4-287 derived from Hernández Lozada *et al*. was synthetized by Twist Biosciences (South San Francisco, CA) and cloned after the P_{EL222} or P_{lacUV5} promoter (Hernández Lozada et al., 2018). Plasmid pBbE5k-P_{EL222}-*Cp*FatB1*-LOVtag was co-transformed with pEL222 for LOVtag + EL222 production control (Table S2).

Plasmids expressing ClpA, ClpX, and HslU were constructed by amplifying the unfoldase gene from the wild type genome and inserting it into the pBbA8k backbone from the BglBrick library (Lee et al., 2011).

Blue light stimulation

Unless otherwise noted, bacteria were cultured in Luria broth (LB) with appropriate antibiotics for plasmid maintenance at 37 °C with 200 rpm shaking. Antibiotic concentrations used for plasmid maintenance were 30 µg/mL for kanamycin, 100 µg/mL for carbenicillin, and 25 µg/mL for chloramphenicol. All light exposure experiments were carried out with a light plate apparatus (LPA) (Gerhardt et al., 2016) using 465 nm blue light. Overnight cultures of light sensitive strains were diluted 1:50 and precultured in the dark for 2 hours. For IPTG inducible constructs, 1mM IPTG was added when the cells were diluted. After 2 hours in the dark, cells were exposed to blue light in the LPA at a setpoint of 100 $\mu W/cm^2$. Red fluorescence (excitation 560 nm, emission 600 nm) and optical density (OD) readings were taken using a BioTek Synergy H1m plate reader (BioTek, Winooski, VT) after 5 hours of incubation. For CRISPRa experiments, light stimulation was continued for 8 hours prior to RFP and OD readings. For frequency response experiments, the LPA was programmed using its Iris software (https://taborlab.github.io/Iris/) to pulse blue light at varying frequencies. A 5 second light pulse was constant for each experiment while the time between pulses was varied (5s, 55s, 85s, 115s, 235s, and 480s).

Minimum inhibitory concentrations

Minimum inhibitory concentration (MIC) experiments for chloramphenicol were performed in M9 minimal media (M9 salts, 2mM $MgSO_4$, 100 μM $CaCl_2$) with 1% glucose at 37 °C with 200 rpm shaking. Overnight cultures in LB were initially diluted 1:50 into M9 media for 4 hours. The M9 conditioned cultures were then diluted again 1:20 into 24 well plates containing M9 media with varying levels of chloramphenicol (0, 0.3125, 0.625, 1.25, 2.5, 5, and 10 μg/ml) and grown for 20 hours before measuring optical density (OD) using a BioTek Synergy H1m plate reader (BioTek, Winooski, VT). We also conducted experiments with the Δ*acrB* strain. For these, Δ*acrB* was transformed with pBbA5k-AcrAB-LOVtag (Table S2) and MIC experiments were carried out either in the LPA with constant light illumination or kept in the dark for the duration of growth. No IPTG was added to the Δ*acrB* + AcrAB-LOVtag cultures because basal expression is enough to recover wild type resistance. The same MIC protocol was performed in the dark using BW25113, Δ*acrB* + AcrB, and un-transformed Δ*acrB* as controls.

Microscopy

Strains were grown overnight in LB medium. Cultures were refreshed 1:100 in M9 minimal media (M9 salts supplemented with 2 mM MgSO4, 0.1 mM CaCl2) with 0.4% glucose for two hours. Samples were then placed on 1.5% low melting agarose pads made with M9 minimal media with 0.4% glucose. Samples were grown at 30°C. Cells were imaged at 100x using a Nikon Ti-E microscope. Blue light exposure was provided by a LED ring (Adafruit NeoPixel 1586), which was fixed above the microscope stage and controlled by an Arduino using a custom Matlab script. Blue light was kept constant except during image acquisitions.

Production experiment

For octanoic acid production experiments, strains expressing *Cp*FatB1* under various modes of control (Table S2) were cultured in LB overnight with light illumination to maintain low *Cp*FatB1* expression. Overnight cultures were diluted 1:20 into M9 minimal media with 2% glucose and kept in the light until they reached an OD_{600} of 0.6 unless otherwise noted. The LPA was then programmed to either maintain light for low octanoic acid production or turn off light exposure to induce octanoic acid production for 24 hours prior to fatty extraction and quantification.

Fatty acid quantification

Samples for GC-MS quantification were taken at 24 hours. 400 μL of vortexed culture was used for fatty acid extraction and derivatization into fatty acid methyl esters as described by Sarria *et al.* (Sarria et al., 2018) with the following minor modifications: An internal standard of nonanoic acid (C9) was added to the 400 μL sample at a final concentration of 88.8 mg/L and vortexed for 5 sec. The following was then added to the sample for fatty acid extraction and vortexed for 30 sec: 50 μL 10% NaCl, 50 μL glacial acetic acid, and 200 μL ethyl acetate. The sample was then centrifuged at 12,000 g for 10 mins. After centrifugation, 100 μL of the ethyl acetate layer was mixed with 900 μL of a 30:1 mixture of methanol:HCl (12N) in a 2 mL microcentrifuge tube. The solution was vortexed for 30 sec followed by an incubation at 50°C for 60 mins for methyl ester derivatization. Once cooled to room temperature, 500 μL hexanes and 500 μL water were added to the 2 mL microcentrifuge tube, vortexed for 10 sec, and allowed to settle. 250 μL of the hexane layer was mixed with 250 μL ethyl acetate in a GC-MS vial for quantification.

The samples were analyzed with an Agilent 6890N/Agilent 5973 MS detector using a DB-5MS column. The inlet temperature was set to 300°C with flow at 4 mL/min. The oven heating program

was initially set to 70°C for 1 min, followed by a ramp to 290°C at 30°C/min, and a final hold at 290°C for 1 min. GLC-20 and GLC-30 FAME standard mixes (Sigma) were tested using this protocol to ensure proper capture of all chain lengths and to gauge retention times. Internal standards were used for quantification, with chain lengths C8-C12 quantified with the nonanoic acid internal standard and C14-C18 quantified with the pentadecanoic internal standard.

Acknowledgements
We thank members of the Dunlop Lab for helpful discussions. This work was supported by DOE grant DE-SC0019387, NSF grant 1804096, and NIH grant R01AI102922. CCO and MBS received support through the NIH training grants T32 GM130546 and T32 EB006359, respectively.

Conflict of Interest
The authors declare no competing interests.

References

Alon U. 2007. Network motifs: Theory and experimental approaches. *Nat Rev Genet* **8**:450–461. doi:10.1038/nrg2102

Andersen JB, Sternberg C, Poulsen LK, Bjørn SP, Givskov M, Molin S. 1998. New unstable variants of green fluorescent protein for studies of transient gene expression in bacteria. *Appl Environ Microbiol* **64**:2240–2246. doi:10.1128/aem.64.6.2240-2246.1998

Baba T, Ara T, Hasegawa M, Takai Y, Okumura Y, Baba M, Datsenko KA, Tomita M, Wanner BL, Mori H. 2006. Construction of Escherichia coli K-12 in-frame, single-gene knockout mutants: The Keio collection. *Mol Syst Biol* **2**. doi:10.1038/msb4100050

Baker TA, Sauer RT. 2006. ATP-dependent proteases of bacteria: recognition logic and operating principles. *Trends Biochem Sci* **31**:647–653. doi:10.1016/j.tibs.2006.10.006

Baumschlager A, Aoki SK, Khammash M. 2017. Dynamic Blue Light-Inducible T7 RNA Polymerases (Opto-T7RNAPs) for Precise Spatiotemporal Gene Expression Control. *ACS Synth Biol* **6**:2157–2167. doi:10.1021/acssynbio.7b00169

Baumschlager A, Rullan M, Khammash M. 2020. Exploiting natural chemical photosensitivity of anhydrotetracycline and tetracycline for dynamic and setpoint chemo-optogenetic control. *Nat Commun* **11**:1–10. doi:10.1038/s41467-020-17677-5

Benzinger D, Ovinnikov S, Khammash M. 2022. Synthetic gene networks recapitulate dynamic signal decoding and differential gene expression. *Cell Syst* **13**:353-364.e6. doi:10.1016/j.cels.2022.02.004

Bondeson DP, Mullin-Bernstein Z, Oliver S, Skipper TA, Atack TC, Bick N, Ching M, Guirguis AA, Kwon J, Langan C, Millson D, Paolella BR, Tran K, Wie SJ, Vazquez F, Tothova Z, Golub TR, Sellers WR, Ianari A. 2022. Systematic profiling of conditional degron tag technologies for target validation studies. *Nat Commun* **13**. doi:10.1038/s41467-022-33246-4

Bonger KM, Rakhit R, Payumo AY, Chen JK, Wandless TJ. 2014. General method for regulating protein stability with light. *ACS Chem Biol* **9**:111–115. doi:10.1021/cb400755b

Cameron DE, Collins JJ. 2014. Tunable protein degradation in bacteria. *Nat Biotechnol* **32**:1276–1281. doi:10.1038/nbt.3053

Chai Q, Wang Z, Webb SR, Dutch RE, Wei Y. 2016. The ssrA-Tag Facilitated Degradation of an Integral Membrane Protein. *Biochemistry* **55**:2301–2304. doi:10.1021/acs.biochem.6b00038

Christie JM, Corchnoy SB, Swartz TE, Hokenson M, Han IS, Briggs WR, Bogomolni RA. 2007. Steric interactions stabilize the signaling state of the LOV2 domain of phototropin 1. *Biochemistry* **46**:9310–9319. doi:10.1021/bi700852w

Chubukov V, Gerosa L, Kochanowski K, Sauer U. 2014. Coordination of microbial metabolism. *Nat Rev Microbiol* **12**:327–340. doi:10.1038/nrmicro3238

Dagliyan O, Tarnawski M, Chu PH, Shirvanyants D, Schlichting I, Dokholyan N V., Hahn KM. 2016. Engineering extrinsic disorder to control protein activity in living cells. *Science (80-)* **354**:1441–1444. doi:10.1126/science.aah3404

Datsenko KA, Wanner BL. 2000. One-step inactivation of chromosomal genes in Escherichia coli K-12 using PCR products. *Proc Natl Acad Sci U S A* **97**:6640–6645. doi:10.1073/pnas.120163297

Deng W, Bates JA, Wei H, Bartoschek MD, Conradt B, Leonhardt H. 2020. Tunable light and drug induced depletion of target proteins. *Nat Commun* **11**:1–13. doi:10.1038/s41467-019-

14160-8
Dessauges C, Mikelson J, Dobrzyński M, Jacques M, Frismantiene A, Gagliardi PA, Khammash M, Pertz O. 2022. Optogenetic actuator – ERK biosensor circuits identify MAPK network nodes that shape ERK dynamics. *Mol Syst Biol* **18**:1–22. doi:10.15252/msb.202110670
Ding Q, Ma D, Liu GQ, Li Y, Guo L, Gao C, Hu G, Ye C, Liu J, Liu L, Chen X. 2020. Light-powered Escherichia coli cell division for chemical production. *Nat Commun* **11**. doi:10.1038/s41467-020-16154-3
Dong C, Fontana J, Patel A, Carothers JM, Zalatan JG. 2018. Synthetic CRISPR-Cas gene activators for transcriptional reprogramming in bacteria. *Nat Commun*. doi:10.1038/s41467-018-04901-6
Du D, Wang Z, James NR, Voss JE, Klimont E, Ohene-Agyei T, Venter H, Chiu W, Luisi BF. 2014. Structure of the AcrAB-TolC multidrug efflux pump. *Nature* **509**:512–515. doi:10.1038/nature13205
Dunlop MJ, Dossani ZY, Szmidt HL, Chu HC, Lee TS, Keasling JD, Hadi MZ, Mukhopadhyay A. 2011. Engineering microbial biofuel tolerance and export using efflux pumps. *Mol Syst Biol* **7**:1–7. doi:10.1038/msb.2011.21
El Meouche I, Dunlop MJ. 2018. Heterogeneity in efflux pump expression predisposes antibiotic-resistant cells to mutation. *Science (80-)* **362**:686–690. doi:10.1126/science.aar7981
Elowitz. 2000. A synthetic oscillatory network repressilator. *Nature* **403**:335–338.
Engler C, Kandzia R, Marillonnet S. 2008. A one pot, one step, precision cloning method with high throughput capability. *PLoS One* **3**:e3647. doi:10.1371/journal.pone.0003647
Fei X, Bell TA, Barkow SR, Baker TA, Sauer RT. 2020. Structural basis of clpxp recognition and unfolding of ssra-tagged substrates. *Elife* **9**:1–39. doi:10.7554/eLife.61496
Finley D. 2009. Recognition and processing of ubiquitin-protein conjugates by the proteasome. *Annu Rev Biochem* **78**:477–513. doi:10.1146/annurev.biochem.78.081507.101607
Fisher MA, Boyarskiy S, Yamada MR, Kong N, Bauer S, Tullman-Ercek D. 2014. Enhancing tolerance to short-chain alcohols by engineering the Escherichia coli AcrB efflux pump to secrete the non-native substrate n-butanol. *ACS Synth Biol* **3**:30–40. doi:10.1021/sb400065q
Flynn JM, Levchenko I, Seidel M, Wickner SH, Sauer RT, Baker TA. 2001. Overlapping recognition determinants within the ssrA degradation tag allow modulation of proteolysis. *Proc Natl Acad Sci U S A* **98**:10584–10589. doi:10.1073/pnas.191375298
Gerhardt KP, Olson EJ, Castillo-Hair SM, Hartsough LA, Landry BP, Ekness F, Yokoo R, Gomez EJ, Ramakrishnan P, Suh J, Savage DF, Tabor JJ. 2016. An open-hardware platform for optogenetics and photobiology. *Sci Rep* **6**:1–13. doi:10.1038/srep35363
Gil AA, Carrasco-López C, Zhu L, Zhao EM, Ravindran PT, Wilson MZ, Goglia AG, Avalos JL, Toettcher JE. 2020. Optogenetic control of protein binding using light-switchable nanobodies. *Nat Commun* **11**:1–12. doi:10.1038/s41467-020-17836-8
Golding I, Paulsson J, Zawilski SM, Cox EC. 2005. Real-time kinetics of gene activity in individual bacteria. *Cell* **123**:1025–1036. doi:10.1016/j.cell.2005.09.031
Gottesman S, Roche E, Zhou YN, Sauer RT. 1998. The ClpXP and ClpAP proteases degrade proteins with carboxy-terminal peptide tails added by the SsrA-tagging system. *Genes Dev* **12**:1338–1347. doi:10.1101/gad.12.9.1338
Guntas G, Hallett RA, Zimmerman SP, Williams T, Yumerefendi H, Bear JE, Kuhlman B. 2015. Engineering an improved light-induced dimer (iLID) for controlling the localization and activity of signaling proteins. *Proc Natl Acad Sci U S A* **112**:112–117.

doi:10.1073/pnas.1417910112
Gupta M, Johnson A, Cruz E, Costa E, Guest R, Li SH-J, Hart EM, Nguyen T, Stadlmeier M, Bratton BP, Silhavy TJ, Wingreen NS, Gitai Z, Wühr M. 2022. Global Protein-Turnover Quantification in Escherichia coli Reveals Cytoplasmic Recycling under Nitrogen-Limitation. *bioRxiv* 2022.08.01.502339.
Gurbatri CR, Lia I, Vincent R, Coker C, Castro S, Treuting PM, Hinchliffe TE, Arpaia N, Danino T. 2020. Engineered probiotics for local tumor delivery of checkpoint blockade nanobodies. *Sci Transl Med* **12**. doi:10.1126/scitranslmed.aax0876
Halavaty AS, Moffat K. 2007. N- and C-terminal flanking regions modulate light-induced signal transduction in the LOV2 domain of the blue light sensor phototropin 1 from Avena sativa. *Biochemistry* **46**:14001–14009. doi:10.1021/bi701543e
Harper SM, Neil LC, Gardner KH. 2003. Structural basis of a phototropin light switch. *Science (80-)* **301**:1541–1544. doi:10.1126/science.1086810
Harrigan P, Madhani HD, El-Samad H. 2018. Real-Time Genetic Compensation Defines the Dynamic Demands of Feedback Control. *Cell* **175**:877-886.e10. doi:10.1016/j.cell.2018.09.044
Hasenjäger S, Trauth J, Hepp S, Goenrich J, Essen LO, Taxis C. 2019. Optogenetic Downregulation of Protein Levels with an Ultrasensitive Switch. *ACS Synth Biol* **8**:1026–1036. doi:10.1021/acssynbio.8b00471
Hernández Lozada NJ, Lai RY, Simmons TR, Thomas KA, Chowdhury R, Maranas CD, Pfleger BF. 2018. Highly Active C8 -Acyl-ACP Thioesterase Variant Isolated by a Synthetic Selection Strategy. *ACS Synth Biol* **7**:2205–2215. doi:10.1021/acssynbio.8b00215
Jayaraman P, Devarajan K, Chua TK, Zhang H, Gunawan E, Poh CL. 2016. Blue light-mediated transcriptional activation and repression of gene expression in bacteria. *Nucleic Acids Res* **44**:6994–7005. doi:10.1093/nar/gkw548
Jõers A, Liske E, Tenson T. 2020. Dividing subpopulation of Escherichia coli in stationary phase. *Res Microbiol* **171**:153–157. doi:10.1016/j.resmic.2020.02.002
Kawano F, Aono Y, Suzuki H, Sato M. 2013. Fluorescence imaging-based high-throughput screening of fast- and slow-cycling LOV proteins. *PLoS One* **8**. doi:10.1371/journal.pone.0082693
Kawano F, Suzuki H, Furuya A, Sato M. 2015. Engineered pairs of distinct photoswitches for optogenetic control of cellular proteins. *Nat Commun*. doi:10.1038/ncomms7256
Keiler KC. 2015. Mechanisms of ribosome rescue in bacteria. *Nat Rev Microbiol* **13**:285–297. doi:10.1038/nrmicro3438
Komera I, Gao C, Guo L, Hu G, Chen X, Liu L. 2022. Bifunctional optogenetic switch for improving shikimic acid production in E. coli. *Biotechnol Biofuels Bioprod* **15**:1–14. doi:10.1186/s13068-022-02111-3
Lalwani MA, Zhao EM, Avalos JL. 2018. Current and future modalities of dynamic control in metabolic engineering. *Curr Opin Biotechnol* **52**:56–65. doi:10.1016/j.copbio.2018.02.007
Lee TS, Krupa RA, Zhang F, Hajimorad M, Holtz WJ, Prasad N, Lee SK, Keasling JD. 2011. BglBrick vectors and datasheets: A synthetic biology platform for gene expression. *J Biol Eng* **5**:12. doi:10.1186/1754-1611-5-12
Li LL, Klein FM, Li Greci L, Popinigis A, Freudenberg F, Courtney MJ. 2020. Resonance energy transfer sensitises and monitors in situ switching of LOV2-based optogenetic actuators. *Nat Commun* **11**:1–18. doi:10.1038/s41467-020-18816-8
Li Y, Zhao M, Wei D, Zhang J, Ren Y. 2022. Photocontrol of Itaconic Acid Synthesis in

Escherichia coli. *ACS Synth Biol* **11**:2080–2088. doi:10.1021/acssynbio.2c00014
Link H, Kochanowski K, Sauer U. 2013. Systematic identification of allosteric protein-metabolite interactions that control enzyme activity in vivo. *Nat Biotechnol* **31**:357–361. doi:10.1038/nbt.2489
Liu J, Chen H, Ma L, He Z, Wang D, Liu Y, Lin Q, Zhang T, Gray N, Kaniskan HÜ, Jin J, Wei W. 2020. Light-induced control of protein destruction by opto-PROTAC. *Sci Adv* **6**:1–12. doi:10.1126/sciadv.aay5154
Lizarralde-Guerrero M, Taraveau F. 2021. Role of AcrAB-TolC multidrug efflux pump in drug-resistance acquisition by plasmid transfer. *Medecine/Sciences* **37**:945–947. doi:10.1051/medsci/2021159
Lugagne JB, Dunlop MJ. 2019. Cell-machine interfaces for characterizing gene regulatory network dynamics. *Curr Opin Syst Biol* **14**:1–8. doi:10.1016/j.coisb.2019.01.001
Lungu OI, Hallett RA, Choi EJ, Aiken MJ, Hahn KM, Kuhlman B. 2012. Designing Photoswitchable Peptides Using the AsLOV2 Domain. *Chem Biol* **19**:507–517. doi:10.1016/j.chembiol.2012.02.006
Mahmoud SA, Chien P. 2018. Regulated Proteolysis in Bacteria. *Annu Rev Biochem* **87**:677–696. doi:10.1146/annurev-biochem-062917-012848
Maier T, Schmidt A, Güell M, Kühner S, Gavin AC, Aebersold R, Serrano L. 2011. Quantification of mRNA and protein and integration with protein turnover in a bacterium. *Mol Syst Biol* **7**:1–12. doi:10.1038/msb.2011.38
Maurizi MR. 1992. Proteases and protein degradation inEscherichia coli. *Experientia* **48**:178–201. doi:10.1007/BF01923511
McGinness KE, Baker TA, Sauer RT. 2006. Engineering Controllable Protein Degradation. *Mol Cell* **22**:701–707. doi:10.1016/j.molcel.2006.04.027
Morreale FE, Kleine S, Leodolter J, Junker S, Hoi DM, Ovchinnikov S, Okun A, Kley J, Kurzbauer R, Junk L, Guha S, Podlesainski D, Kazmaier U, Boehmelt G, Weinstabl H, Rumpel K, Schmiedel VM, Hartl M, Haselbach D, Meinhart A, Kaiser M, Clausen T. 2022. BacPROTACs mediate targeted protein degradation in bacteria. *Cell* **185**:2338-2353.e18. doi:10.1016/j.cell.2022.05.009
Nagar N, Ecker N, Loewenthal G, Avram O, Ben-Meir D, Biran D, Ron E, Pupko T. 2021. Harnessing Machine Learning To Unravel Protein Degradation in Escherichia coli. *mSystems* **6**. doi:10.1128/msystems.01296-20
Nihongaki Y, Kawano F, Nakajima T, Sato M. 2015. Photoactivatable CRISPR-Cas9 for optogenetic genome editing. *Nat Biotechnol* **33**:755–760. doi:10.1038/nbt.3245
Okusu H, Ma D, Nikaido H. 1996. AcrAB efflux pump plays a major role in the antibiotic resistance phenotype of Escherichia coli multiple-antibiotic-resistance (Mar) mutants. *J Bacteriol* **178**:306–308. doi:10.1128/jb.178.1.306-308.1996
Olson EJ, Hartsough LA, Landry BP, Shroff R, Tabor JJ. 2014. Characterizing bacterial gene circuit dynamics with optically programmed gene expression signals. *Nat Methods* **11**:449–455. doi:10.1038/nmeth.2884
Pudasaini A, El-Arab KK, Zoltowski BD. 2015. LOV-based optogenetic devices: Light-driven modules to impart photoregulated control of cellular signaling. *Front Mol Biosci* **2**:1–15. doi:10.3389/fmolb.2015.00018
Renicke C, Schuster D, Usherenko S, Essen LO, Taxis C. 2013. A LOV2 domain-based optogenetic tool to control protein degradation and cellular function. *Chem Biol* **20**:619–626. doi:10.1016/j.chembiol.2013.03.005

Sarria S, Bartholow TG, Verga A, Burkart MD, Peralta-Yahya P. 2018. Matching Protein Interfaces for Improved Medium-Chain Fatty Acid Production. *ACS Synth Biol* **7**:1179–1187. doi:10.1021/acssynbio.7b00334

Sarria S, Kruyer NS, Peralta-Yahya P. 2017. Microbial synthesis of medium-chain chemicals from renewables. *Nat Biotechnol* **35**:1158–1166. doi:10.1038/nbt.4022

Schrader EK, Harstad KG, Matouschek A. 2009. Targeting proteins for degradation. *Nat Chem Biol* **5**:815–822. doi:10.1038/nchembio.250

Shin J, Zhang S, Der BS, Nielsen AA, Voigt CA. 2020. Programming Escherichia coli to function as a digital display . *Mol Syst Biol* **16**:1–12. doi:10.15252/msb.20199401

Stricker J, Cookson S, Bennett MR, Mather WH, Tsimring LS, Hasty J. 2008. A fast, robust and tunable synthetic gene oscillator. *Nature* **456**:516–519. doi:10.1038/nature07389

Strickland D, Lin Y, Wagner E, Hope CM, Zayner J, Antoniou C, Sosnick TR, Weiss EL, Glotzer M. 2012. TULIPs: Tunable, light-controlled interacting protein tags for cell biology. *Nat Methods* **9**:379–384. doi:10.1038/nmeth.1904

Strickland D, Moffat K, Sosnick TR. 2008. Light-activated DNA binding in a designed allosteric protein. *Proc Natl Acad Sci U S A* **105**:10709–10714. doi:10.1073/pnas.0709610105

Strickland D, Yao X, Gawlak G, Rosen MK, Gardner KH, Sosnick TR. 2010. Rationally improving LOV domain-based photoswitches. *Nat Methods* **7**:623–626. doi:10.1038/nmeth.1473

Striebel F, Kress W, Weber-Ban E. 2009. Controlled destruction: AAA+ ATPases in protein degradation from bacteria to eukaryotes. *Curr Opin Struct Biol* **19**:209–217. doi:10.1016/j.sbi.2009.02.006

Swartz TE, Corchnoy SB, Christie JM, Lewis JW, Szundi I, Briggs WR, Bogomolni RA. 2001. The Photocycle of a Flavin-binding Domain of the Blue Light Photoreceptor Phototropin. *J Biol Chem* **276**:36493–36500. doi:10.1074/jbc.M103114200

Szydlo K, Ignatova Z, Gorochowski TE. 2022. Improving the Robustness of Engineered Bacteria to Nutrient Stress Using Programmed Proteolysis. *ACS Synth Biol* **11**:1049–1059. doi:10.1021/acssynbio.1c00490

Teelucksingh T, Thompson LK, Zhu S, Kuehfuss NM, Goetz JA, Gilbert SE, MacNair CR, Geddes-McAlister J, Brown ED, Cox G. 2022. A genetic platform to investigate the functions of bacterial drug efflux pumps. *Nat Chem Biol*. doi:10.1038/s41589-022-01119-y

Torella JP, Ford TJ, Kim SN, Chen AM, Way JC, Silver PA. 2013. Tailored fatty acid synthesis via dynamic control of fatty acid elongation. *Proc Natl Acad Sci U S A* **110**:11290–11295. doi:10.1073/pnas.1307129110

Trauth J, Scheffer J, Hasenjäger S, Taxis C. 2019. Synthetic Control of Protein Degradation during Cell Proliferation and Developmental Processes. *ACS Omega* **4**:2766–2778. doi:10.1021/acsomega.8b03011

Turner WJ, Dunlop MJ. 2015. Trade-Offs in Improving Biofuel Tolerance Using Combinations of Efflux Pumps. *ACS Synth Biol* **4**:1056–1063. doi:10.1021/sb500307w

Wang H, Vilela M, Winkler A, Tarnawski M, Schlichting I, Yumerefendi H, Kuhlman B, Liu R, Danuser G, Hahn KM. 2016. LOVTRAP: An optogenetic system for photoinduced protein dissociation. *Nat Methods* **13**:755–758. doi:10.1038/nmeth.3926

Wang T, Tague N, Whelan SA, Dunlop MJ. 2021. Programmable gene regulation for metabolic engineering using decoy transcription factor binding sites. *Nucleic Acids Res* **49**:1163–1172. doi:10.1093/nar/gkaa1234

Xue G, Wang K, Zhou D, Zhong H, Pan Z. 2019. Light-Induced Protein Degradation with

Photocaged PROTACs. *J Am Chem Soc* **141**:18370–18374. doi:10.1021/jacs.9b06422
Yamamoto A, Iwata T, Sato Y, Matsuoka D, Tokutomi S, Kandori H. 2009. Light signal transduction pathway from flavin chromophore to the Jα helix of Arabidopsis phototropin1. *Biophys J* **96**:2771–2778. doi:10.1016/j.bpj.2008.12.3924
Yao X, Rosen MK, Gardner KH. 2008. Estimation of the available free energy in a LOV2-Jα photoswitch. *Nat Chem Biol* **4**:491–497. doi:10.1038/nchembio.99
Ye Z, Li S, Hennigan JN, Lebeau J, Moreb EA, Wolf J, Lynch MD. 2021. Two-stage dynamic deregulation of metabolism improves process robustness & scalability in engineered E. coli. *Metab Eng* **68**:106–118. doi:10.1016/j.ymben.2021.09.009
Yumerefendi H, Wang H, Dickinson DJ, Lerner AM, Malkus P, Goldstein B, Hahn K, Kuhlman B. 2018. Light-Dependent Cytoplasmic Recruitment Enhances the Dynamic Range of a Nuclear Import Photoswitch. *ChemBioChem* **19**:1319–1325. doi:10.1002/cbic.201700681
Zayner JP, Antoniou C, French AR, Hause RJ, Sosnick TR. 2013. Investigating models of protein function and allostery with a widespread mutational analysis of a light-activated protein. *Biophys J* **105**:1027–1036. doi:10.1016/j.bpj.2013.07.010
Zoltowski BD, Motta-Mena LB, Gardner KH. 2013. Blue light-induced dimerization of a bacterial LOV-HTH DNA-binding protein. *Biochemistry* **52**:6653–6661. doi:10.1021/bi401040m
Zoltowski BD, Vaccaro B, Crane BR. 2009. Mechanism-based tuning of a LOV domain photoreceptor. *Nat Chem Biol* **5**. doi:10.1038/nchembio.210

Figures

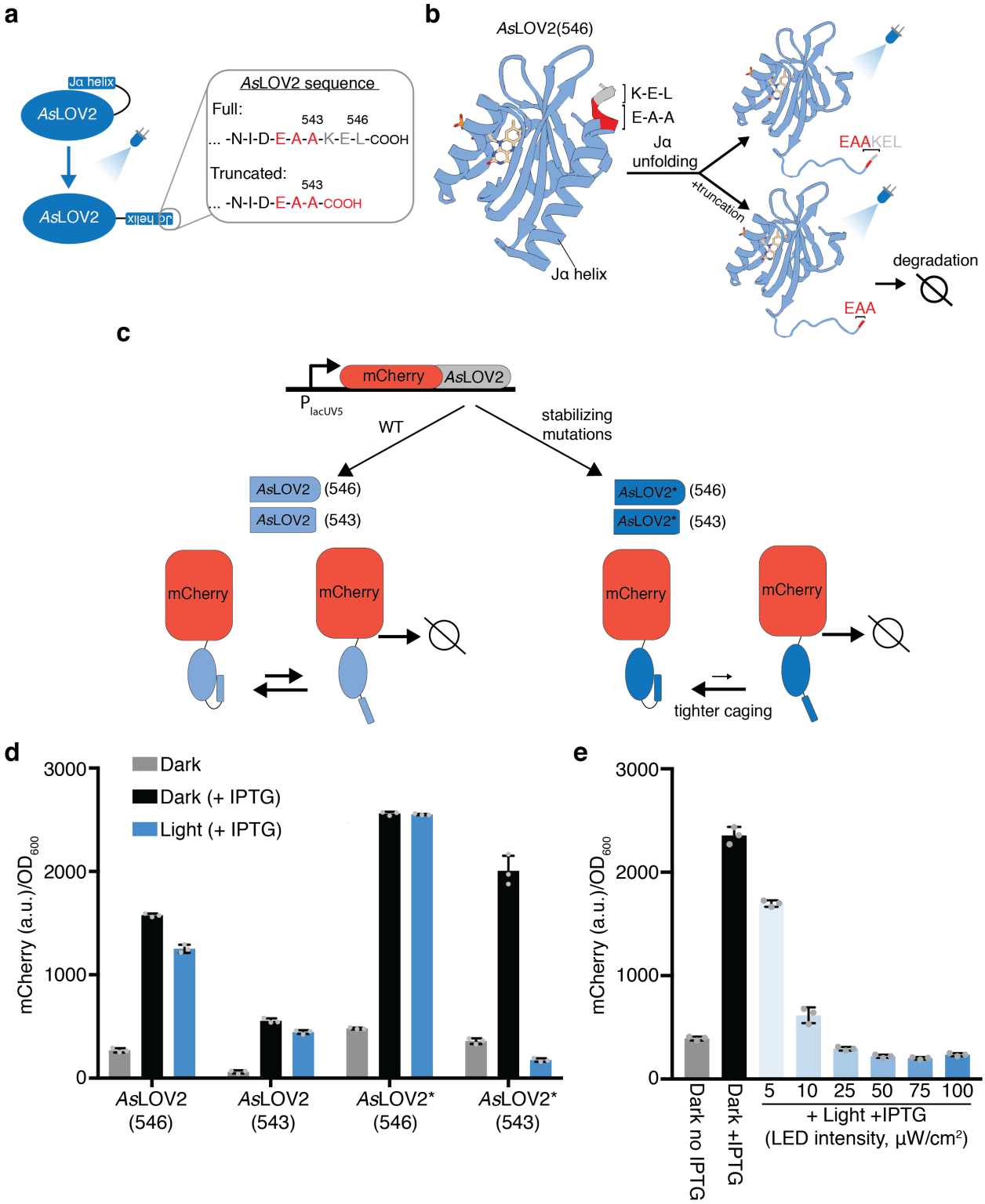
a
Jα helix
AsLOV2
AsLOV2
Jα helix
AsLOV2 sequence
Full:
543 546
... -N-I-D-E-A-A-K-E-L-COOH
Truncated:
543
... -N-I-D-E-A-A-COOH
b
AsLOV2(546)
K-E-L
E-A-A
Jα
unfolding
+truncation
EAAKEL
EAA
degradation
Jα helix
c
mCherry
AsLOV2
P lacUV5
WT
stabilizing
mutations
AsLOV2 (546)
AsLOV2 (543)
AsLOV2* (546)
AsLOV2* (543)
mCherry
tighter caging
d
Dark
Dark (+ IPTG)
Light (+ IPTG)
mCherry (a.u.)/OD600
3000
2000
1000
0
AsLOV2 (546)
AsLOV2 (543)
AsLOV2* (546)
AsLOV2* (543)
e
mCherry (a.u.)/OD600
Dark no IPTG
Dark +IPTG
5 10 25 50 75 100
+ Light +IPTG
(LED intensity, μW/cm2)

Figure 1. Design of *As*LOV2-based degradation tag. **(a)** Primary sequence of *As*LOV2(546) C-terminal sequence. A three amino acid truncation exposes E-A-A. **(b)** Structure of *As*LOV2 (aa404-546, PDB: 2V1A). Amino acids 541-543 (E-A-A) are red and 544-546 (K-E-L) are gray at the C-terminal of the Jα helix. **(c)** Construct used to characterize optogenetic control using *As*LOV2 variants. Each variant is translationally fused to mCherry expressed from an IPTG inducible promoter. Variants include wild type *As*LOV2 (light blue) and a dark state stabilized version, AsLOV2* (dark blue), with and without the three amino acid truncation. **(d)** mCherry expression levels in response to 465 nm blue light for wild type *As*LOV2 and mutated *As*LOV2* fusions with and without truncation. **(e)** Expression of mCherry-LOVtag in response to variable light intensities. Error bars show standard deviation around the mean (n = 3 biological replicates).

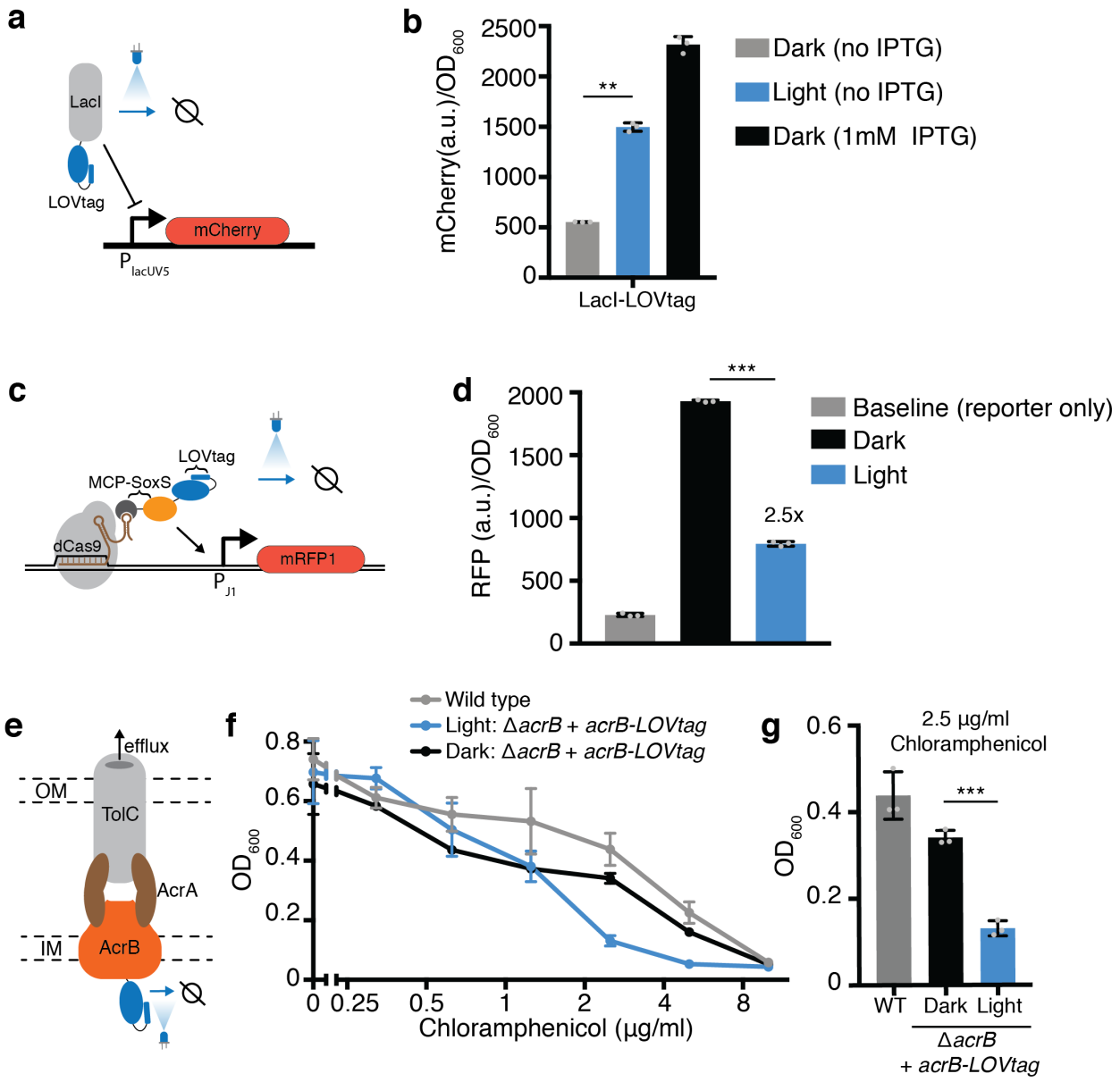

Figure 2. Incorporating light responsiveness into diverse proteins with the LOVtag. **(a)** Control of mCherry repression using a LacI-LOVtag fusion. **(b)** mCherry expression in response to light exposure for strains with LacI-LOVtag compared to IPTG induction (**$p < 0.001$, two tailed unpaired t-test). **(c)** Schematic of SoxS-based CRISPRa activation with a LOVtag appended to the MCP-SoxS activator. **(d)** CRISPRa control of mRFP1 expression in response to light (***$p < 0.0001$, two tailed unpaired t-test). **(e)** Schematic of the LOVtag appended to AcrB of the AcrAB-TolC efflux pump. IM, inner membrane; OM, outer membrane. **(f)** Minimum inhibitory concentration (MIC) curves of cells cultured in chloramphenicol. Wild type cells (BW25113) are compared to a Δ*acrB* strain complemented with AcrB-LOVtag and exposed to light or kept in the dark. **(g)** OD_{600} of strains shown in (f) at 2.5 μg/ml chloramphenicol (***$p < 0.0001$, two tailed unpaired t-test). Error bars show standard deviation around the mean (n = 3 biological replicates).

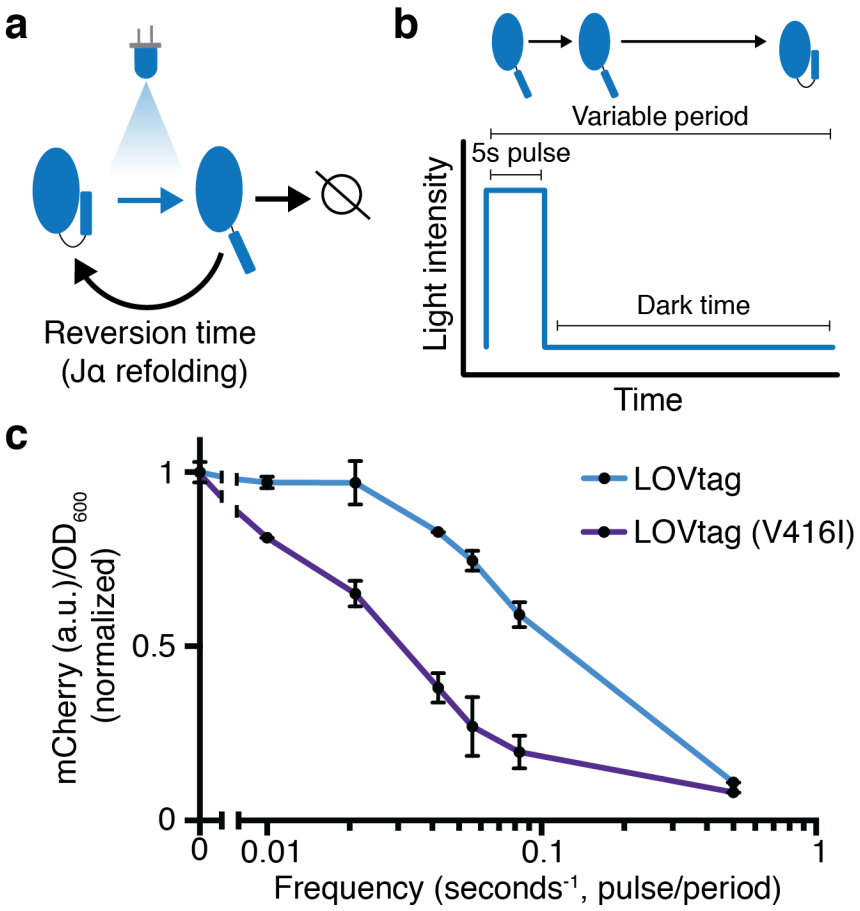

Figure 3. Modulating LOVtag frequency response with photocycle mutations. **(a)** Photocycle of *As*LOV2. Upon light absorption, the Jα helix unfolds for a period of time dictated by stability of the light state conformation. If not degraded, the Jα helix refolds, blocking degradation. **(b)** The light program used to test frequency responses of LOVtag photocycle variants in (c). A constant pulse of 5 sec is followed by a variable dark time that allows for Jα helix refolding. **(c)** Expression of mCherry-LOVtag and variant mCherry-LOVtag (V416I) in response to different frequencies of blue light pulses. Fluorescent values are normalized to dark state expression. Error bars show standard deviation around the mean (n = 3 biological replicates).

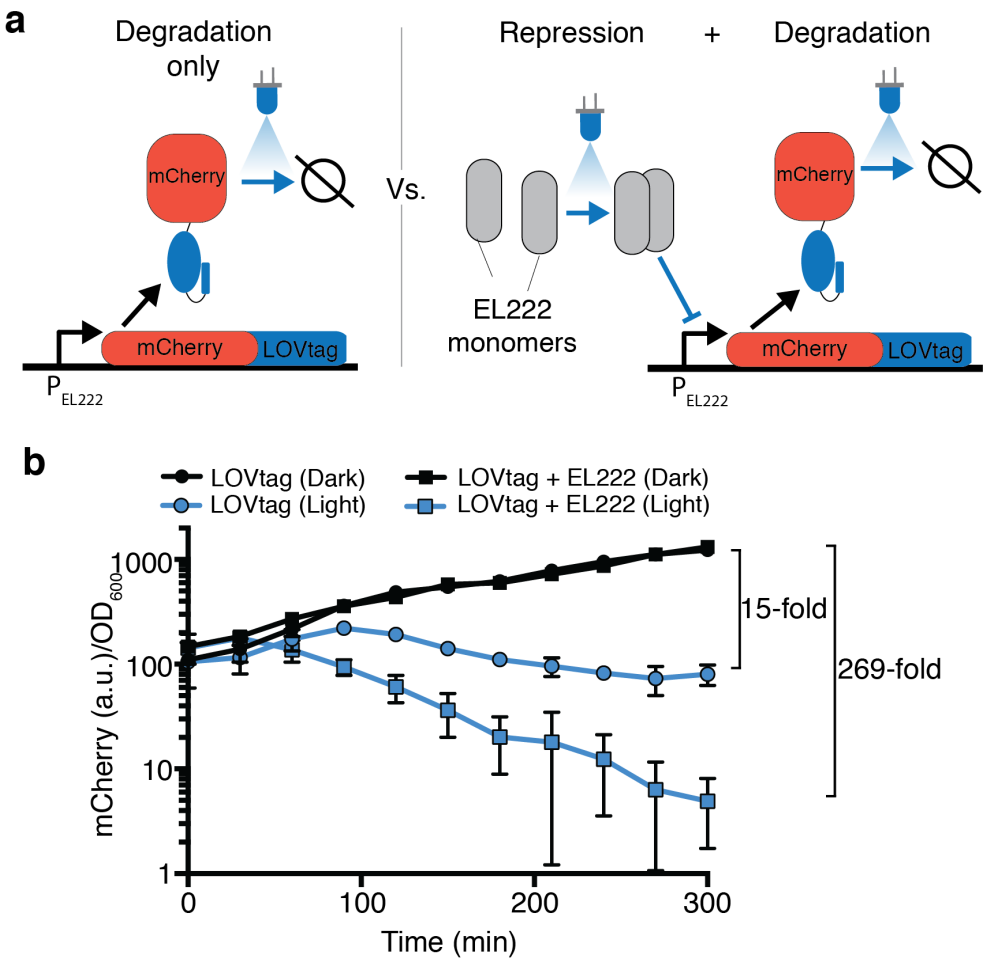

Figure 4. Enhanced light response using transcriptional control together with the LOVtag. **(a)** The mCherry-LOVtag expressed from an EL222 responsive promoter that is constitutively active in the absence of EL222. Addition of EL222 results in a circuit that both represses and degrades in response to light. **(b)** Light and dark expression of mCherry in the 'degradation only' (circles) or 'repression + degradation' (squares) strains from (a) over time. Error bars show standard deviation around the mean (n = 3 biological replicates).

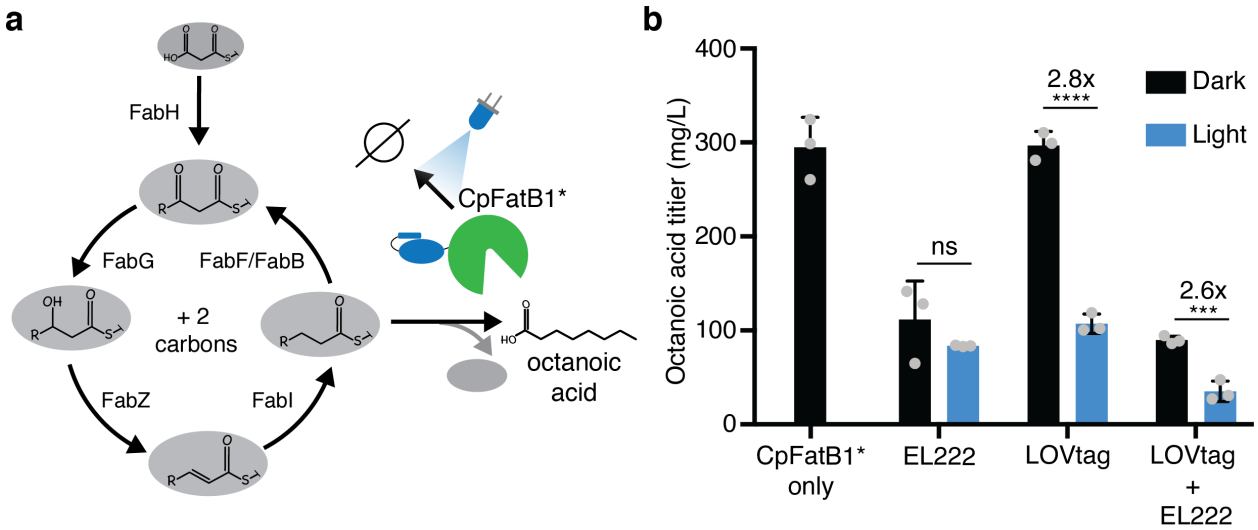

Figure 5. Optogenetic control of octanoic acid production. **(a)** Schematic of fatty acid synthesis in *E. coli*. *Cp*FatB1* catalyzes elongating C8-ACP molecules from this pathway to produce free octanoic acid. *Cp*FatB1* is tagged with a LOVtag to create optogenetic control. **(b)** Octanoic acid titer from strains that express EL222 only, *Cp*FatB1*-LOVtag only, or *Cp*FatB1*-LOVtag + EL222 control measured by GC-MS. Strains were kept either in the dark or with continuous blue light exposure for the duration of the production period. Error bars show standard deviation around the mean (****$p < 0.0001$; ***$p < 0.0001$; n.s., not significant; two tailed unpaired t-test; n = 3 biological replicates)**.**